www.czasopisma.pan.pl PAN www.journals.pan.pl
Opto-Electronics Review 26 (2018) 210–216

Contents lists available at ScienceDirect

Opto-Electronics Review

journal homepage: http://www.journals.elsevier.com/opto-electronics review

Full Length Article

Optimization of optical characteristics of $In_{0.29}Ga_{0.71}As_{0.99}N_{0.01}$/GaAs straddled nano-heterostructure

K. Sandhya [a], G. Bhardwaj [b], R. Dolia [b], P. Lal [a], S. Kumar [c], S. Dalela [d], F. Rahman [e], P.A. Alvi [a,*]

[a] Department of Physics, Banasthali Vidyapith, Banasthali, 304022, Rajasthan, India
[b] Department of Electronics, Banasthali Vidyapith, Banasthali, 304022, Rajasthan, India
[c] Electronic Materials & Nanomagnetism Lab, Department of Applied Physics, Amity School of Applied Sciences, Amity University Haryana, Gurgaon, 122413, India
[d] Department of Pure & Applied Physics, University of Kota, Kota, Rajasthan, India
[e] Department of Physics, Aligarh Muslim University, Aligarh, 202002, U.P, India

ARTICLE INFO

Article history:
Received 30 November 2017
Received in revised form 2 April 2018
Accepted 9 June 2018
Available online 11 July 2018

Keywords:
InGaAsN
Optical gain
Gain compression
Heterostructure

ABSTRACT

Designing of a nanoscale Quantum Well (QW) heterostructure with a well thickness of ~60 Å is critical for many applications and remains a challenge. This paper has a detailed study directed towards designing of $In_{0.29}Ga_{0.71}As_{0.99}N_{0.01}$/GaAs straddled nanoscale-heterostructure having a single QW of thickness ~60 Å and optimization of optical and lasing characteristics such as optical and mode gain, differential gain, gain compression, anti-guiding factor, transparency wavelength, relaxation oscillation frequency (ROF), optical power and their mutual variation behavior. The outcomes of the simulation study imply that for the carrier concentration of $\sim 2 \times 10^{18}\,cm^{-3}$ the optical gain of the nano-heterostructure is of $2100\,cm^{-1}$ at the wavelength is of 1.30 μm. Though the obtained gain is almost half of the gain of InGaAlAs/InP heterostructure, but from the wavelength point of view the InGaAsN/GaAs nano-heterostructure is also more desirable because the 1.30 μm wavelength is attractive due to negligible dispersion in the silica based optical fiber. Hence, the InGaAsN/GaAs nano-heterostructure can be very valuable in optical fiber based communication systems.

1. Introduction

Recently, III-Nitride compound semiconductors based heterostructures, especially nano-scaled heterostructures, have attracted researchers belonging to optoelectronic community due to their potential applications such as light emitting diodes (LEDs), field effect transistors [1–4], detectors, solar cells and laser diodes [5,6]. Nano-heterostructures are ubiquitous of nano-semiconductor devices and have brought drastic changes in our routine life and are considered as heart for optoelectronic devices. The III-nitride based semiconductors, for examples: GaN, InN, AlN and their alloys, have been found to provide unique electrical, electronic, optical and mechanical properties which can be utilized for designing of future photonic and optoelectronic devices [7–9]. Since these semiconductors have wide band gap ranging from 1.9 eV to 6.2 eV, and, therefore, these materials can be used in the fabrication of optoelectronic devices operating in visible-to-ultraviolet regime. Examples are green, blue lasers and photo detectors. To date, III-nitrides based photodetectors operating in ultraviolet regime have exhibited promising output. In addition, III-nitrides based LEDs have been commercialized due to emission of a super bright blue and green light. Moreover, these materials have some exceptional physical properties which make the devices ready for applications beyond the data storage and imaging [10]. These materials are also useful in high temperature electronics and space applications because these are physically and chemically strong. This property makes them ideal for operation in cruel environment.

For the last three decades a lot of experimental and theoretical work has been carried out on III-nitride heterostructures and demonstrated their working with efficient characteristics successfully. For example, in 1982, first time Yoshida *et al.* [11] had fabricated GaN/AlN heterostructure and demonstrated that by using AlN buffer layer the cathode luminescence efficiency of the overlaying GaN could be improved. The main success in the history of III-nitride materials was achieved by a p-type doping in a GaN technology. Since, in general the n-type doping has been much easier than the p-type doping in these materials. The reason behind this fact is that the III-nitride materials have the tendency to show the n-type conductivity during their growth. The n-type doping in

* Corresponding author.
E-mail address: aparvez@banasthali.in (P.A. Alvi).

https://doi.org/10.1016/j.opelre.2018.06.003
1230-3402/

GaN has been incorporated using Ge, Si, S, and Se; while the p-type doping in GaN, InGaN and AlGaN has been achieved using Mg. Since the doping mechanism is very sensitive to dopant flow rate, hence the doping control is not so easy and, therefore, requires full attention of researchers during growth of these materials and in near future much more research work is needed in this direction.

Thus, using the p-type doping technology in 1993 for the first time Nakamura [12] had fabricated heterostructure based p-GaN/n-InGaN/n-GaN blue LEDs and was awarded by Nobel Prize for this work in 2014. Nakamura *et al.* [13]. demonstrated, in 1996, first violet laser which was based on InGaN/GaN/AlGaN heterostructures. In 1994, Khan *et al.* [14]. demonstrated the first breakthrough of high mobility transistors based on AlGaN/GaN heterostructure. Thus, prior to realize these devices, growth of device quality epilayers, study, and fabrication of heterostructures are required. Several groups have reported high quality InGaN/GaN multi quantum well (MQW) system grown by MBE (Molecular Beam Epitaxy). The MQW based heterostructure of InGaN/GaN material system with different indium mole fractions having 10-periods has been reported by Shen *et al.* [15]. Again, the MQW based heterostructure of InGaN/GaN material system with abrupt interfaces between wells and barriers was reported by Ng *et al.* [16]. In 2006, the heterostructures of InN/InGaN material system having 20 MQWs have been fabricated using radio frequency PAMBE (plasma assisted molecular beam epitaxiy) and reported by Che *et al.* [17]. Among other IIII-nitride based heterostructures, the InN/GaN material based heterostructures have several advantages in the area THz (Tera Hertz) electronic devices operating in THz region [18]. The main advantages are: high emission rate of optical phonon ($\sim 2.5 \times 10^{13}$ s^{-1}), high thermal conductivity, very high electron drift velocity ($\sim 5 \times 10^7$ cm s^{-1}) in InN and large conduction band offset value which ensures the blocking of the conduction current over the barriers of the heterostructures [18,19]. But, there is one disadvantage of these semiconductors is that they have high effective masses in comparison to conventional semiconductors and, thus they have low carrier's mobility; but this drawback is compensated by the high electron drift velocity exhibited by these materials.

From the application point of view, III-nitride materials based devices are more beneficial in comparison to conventional semiconducting materials. For example, III-nitride materials based UV photodetectors are much sensitive to ultraviolet radiations while insensitive to infrared radiation. Thus, these devices are applicable in order to detect the ultraviolet radiations existing in the infrared and visible background [20]. Due to this, the III-nitride devices can be utilized in engine and furnace monitoring for automotive, flame detection, undersea communication, petroleum industry, and space-to-space communication, and in chemical analysis systems. One of the major advantages is that the III-nitride devices can be expected to work without optical filters due to their low dark currents and theoretical intrinsic solar blindness and, obviously, this behaviour of these devices reduce the launch weight for space significantly.

In the recent decade, a lot of progress on III-nitride material based semiconducting heterostructures has been reported focusing, particularly, on their usage. For example, nitride heterojunctions based tandem solar cells have been reported for their maximum conversion efficiency up to 45% [21]. Also, the dilute nitride based heterostructures have been found in form of a strong device for the development of frequency-doubled high brightness laser sources which can emit red-orange radiations [22,23]. Such device could be developed with the help of technological advancement of a high-quality fabrication of dilute nitride gain mirrors giving photonic emission at 1220–1240 nm wavelengths [24]. In the last decade, Riechert *et al.* [25]. have reported growth mechanism of a type-I InGaAsN/GaAs heterostructure along with its some electrical properties but have not studied optical properties in detail.

The aim of this paper is to focus on optical properties along with some electrical characteristics of a straddled (or type-I) InGaAsN/GaAs material based nano-heterostructure. In order to study the optical characteristics of the heterostructure such as optical gain, mode gain, differential gain and gain compression, the mechanism of conduction and valence band has been studied by studying the behaviour of the envelope functions or wavefunctions associated with the respective bands lying in the active region of the heterostructure by making use of **k.p** method within the frame work of GAIN simulation package.

2. Device's structural detail and supported theory

The device structure of InGaAsN/GaAs material system is very simple and has type-I (straddled type) heterostructure, in which the band gap of the sandwiched material (active region) has been considered very small in comparison to the barrier region. For the formation of active region (quantum well) in the heterostructure, InGaAsN quaternary material has been selected keeping in view its band gap and, hence the operating wavelength of the heterostructure. The active region of the device sandwiched between two barriers followed by claddings. The barriers and claddings are considered of GaAsN (with dilute N) material. The width of active region (quantum well region) is taken as 60 Å; while barriers are of width ~50 Å. The details of design parameters are listed in Table 1. Here, the size of active region is approximately comparable to the de-Broglie wavelength. The region behind the chosen of such size of active region is to have quantum confinement of the envelope function (or wave function) associated with the quantum well. Because, for the quantum mechanical observations such as optical emission or optical absorption, the size of the active region should be comparable to the de-Broglie wavelength. The entire device is supposed to grow on a GaAs substrate. The choice of the GaAs substrate for such a device is preferred so that the lattice constant of the active region material can be matched with lattice constant of substrate and, hence lattice matched condition of a quantum well with the substrate could be maintained in order to avoid unnecessary strain in the device. The unnecessary strain produced in the device may degrade the device performance. For example, in a recent work, type-I InGaAs/GaAsP nano-heterostructure grown pseudomorphically on GaAs substrate (in which InGaAs material is lattice matched with GaAs substrate) has been found to exhibit good performance [26].

In order to optimize the optical properties of the heterostructure, use of basic quantum mechanics has been done. For the conduction band analysis, initially it is assumed that the conduction band of the active region is semi-parabolic and with this assumption the Schrödinger equation is solved to find out the wavefunctions of electrons in conductions band and their corresponding discrete energies (conduction subbands). For understanding the mechanism of valence band, **k.p** method is utilized. An 8×8 Kohn-Luttinger Hamiltonian is solved to obtain the wavefunctions associated with the valence subbands and their corresponding discrete energies, i.e., heavy and light holes' energies. The calculated energy values of electrons and holes are mentioned in Table 2. To perform such calculations, a particular simulation package (GAIN) has been utilized which works in the vicinity of the zone centre at the Γ point. The limitation of this software is that it does work only for III-V semiconducting materials and particularly for direct semiconductors that's why the Γ point is chosen. It may be noted that in these calculations the split-off (SO holes) subbands have been neglected because their position is found to lie much below the top of the valence band.

Table 1
Design parameters of InGaAsN QW Heterostructure.

Role of Layer	Layers Specification	Layers Thickness (Å)	Lattice constants (Å)	Strain	Conduction band edge-offset (eV)	Valence band edge-offset (eV)
Quantum well	$In_{0.29}Ga_{0.71}As_{0.99}N_{0.01}$	60	5.766	−0.020	0.1076888	−0.0538444
Barrier	$GaAs_{0.10}N_{0.90}$	50	6.017	−0.060	0.3450696	−0.1478870
Cladding	$GaAs_{0.41}N_{0.59}$	100	5.892	−0.040	0.7036184	−0.3015508
Substrate	GaAs	–	5.653	–	–	–

Table 2
Energies values of the electrons and holes.

CONDUCTION BAND ELECTRON ENERGIES	VALENCE SUBBAND ENERGIES
Energy of first electronic state: 0.178 eV	**For Heavy Holes (HH)**
Energy of second electronic state: 0.349 eV	Energy of first hole (HH) state: 0.867 eV
Energy of third electronic state: 0.451 eV	Energy of second hole (HH) state: -0.122 eV
Energy of fourth electronic state: 0.529 eV	Energy of third hole (HH) state: -0.167 eV
Energy of fifth electronic state: 0.690 eV	Energy of fourth hole (HH) state: -0.178 eV
	Energy of fifth hole (HH) state: -0.218 eV
	Energy of sixth hole (HH) state: -0.252 eV
	For Light Holes (LH)
	Energy of first hole (LH) state: -0.150 eV
	Energy of second hole (LH) state: -0.190 eV
	Energy of third hole (LH) state: -0.240 eV
	Energy of fourth hole (LH) state: -0.297 eV

The optical gain (within both TE and TM modes) in the designed heterostructure can be simulated by the following expression of optical gain [27–30]:

$$G(\hbar\omega) = \frac{\pi e^2}{nc\varepsilon\omega Lm^2} \sum_{\eta=\uparrow,\downarrow} \sum_{\sigma=U,L} \sum_{n,m} \int \left|\left(\hat{e}.M_{nm}^{\eta\sigma}(k_t)\right)\right|^2 \times \frac{\left(f_n^c(k_t) - f_{\sigma m}^v(k_t)\right)\left(\frac{\gamma}{\pi}\right)}{\left(E_{\eta,\sigma nm}^{c,v}(k_t) - \omega\hbar\right)^2 + \gamma^2} \frac{k_t dk_t}{2\pi} \quad \text{(i)}$$

where the symbols used in the above expression have been explained very well in Refs. [27]27, [30]30, and [31]31.

Since in the present work, the heterostructure designed under study is symmetric, hence for a symmetrical structure, the optical gain will be modified as;

$$G(\hbar\omega) = \frac{2.\pi e^2}{nc\varepsilon\omega Lm^2} \sum_{\sigma=U,L} \sum_{n,m} \int \left|\left(\hat{e}.M_{nm}^{\eta\sigma}(k_t)\right)\right|^2 \times \frac{\left(f_n^c(k_t) - f_{\sigma m}^v(k_t)\right)\left(\frac{\gamma}{\pi}\right)}{\left(E_{\eta,\sigma nm}^{c,v}(k_t) - \omega\hbar\right)^2 + \gamma^2} \frac{k_t dk_t}{2\pi} \quad \text{(ii)}$$

The appearance of the factor 2 in the above formula has replaced the sum over σ for the holes' spins in the valence band only.

The anti-guiding factor (α), which support gain characteristics of the heterostructure, can be determined by the expression as $\alpha = 4\pi(-n')/\lambda G'$; where n' and G' are the differential gain and differential refractive index change with respect to carrier concentration, respectively, in the nano-heterostructure, λ is the lasing wavelength.

3. Results and discussions

The study of quasi Fermi levels is an essential requirement to explain the behaviour of optical gain in the QW Straddled type heterostructures. Under the non equilibrium cases, these quasi Fermi levels play a very important role in specifying the carrier concentrations in the heterostructure. The separation between quasi Fermi energy levels plays a critical role in the semiconducting heterostructure because of its relationship with the density of injected carriers and the intensity of optical gain [32]. In order to achieve the optical gain in the proposed heterostructure, the separation between the quasi Fermi levels must be greater than the energy band gap of the material of the quantum well within the heterostructure. In a better explanation, the separation between Fermi levels equal to energy band gap of the quantum well region can be referred as the transparency condition that results into zero optical gain. On the other hand, if the separation between Fermi levels is less than the band gap, then the resulting optical gain becomes negative and can be referred as optical loss. In Fig. 1, the behaviour of quasi Fermi levels for electrons in the conduction and holes in the valence bands in the left (black) and right (blue) y-axes, respectively, is shown for $In_{0.29}Ga_{0.71}As_{0.99}N_{0.01}$/GaAs straddled heterostructures. Figure 1 predicts that quasi Fermi energies for both the conduction and valence bands are increased as an increase in carrier density. Moreover, the separation between both the quasi Fermi levels is also increased as an increase in carrier densities. Thus, this separation has a crucial role in the existence of optical gain in the proposed straddled heterostructures.

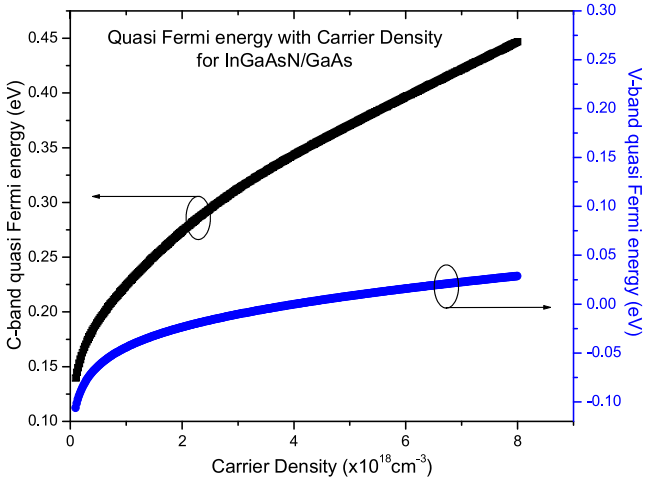

Fig. 1. Conduction and valence bands quasi Fermi levels as a function of Carrier density for $In_{0.29}Ga_{0.71}As_{0.99}N_{0.01}$/GaAs straddled heterostructures.

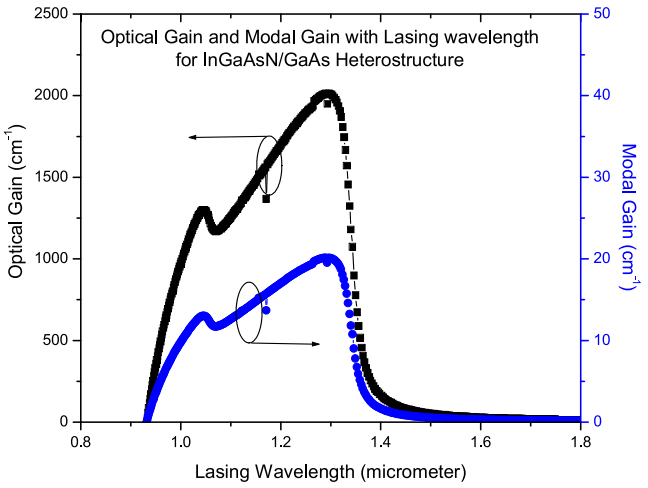

Fig. 2. Optical gain and Modal gain with Lasing wavelength for $In_{0.29}Ga_{0.71}As_{0.99}N_{0.01}$/GaAs straddled heterostructures.

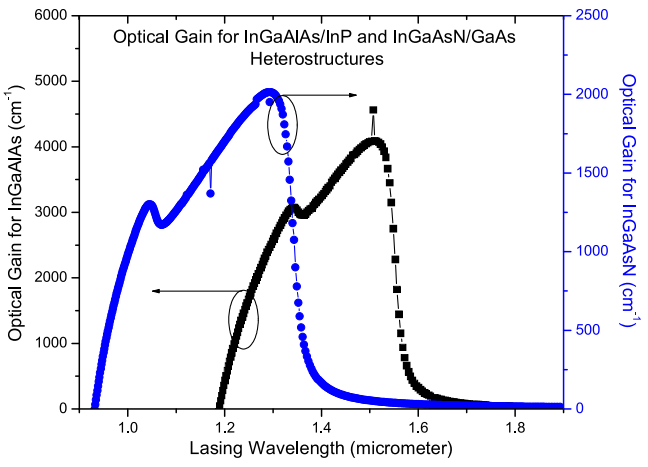

Fig. 3. Optical gain with Lasing wavelength for InGaAlAs/InP and $In_{0.29}Ga_{0.71}As_{0.99}N_{0.01}$/GaAs straddled heterostructures.

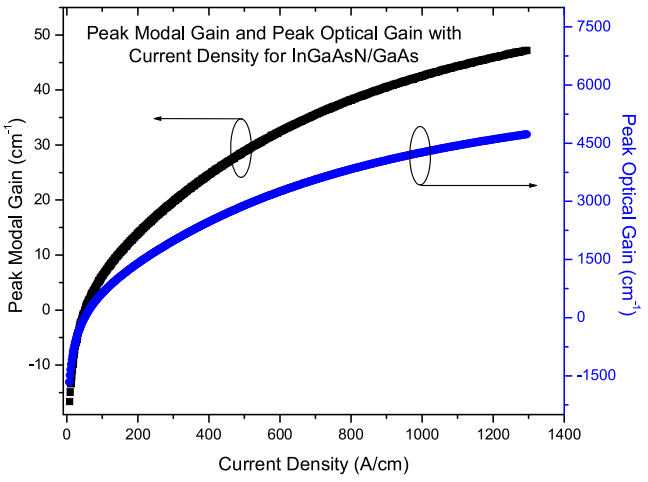

Fig. 4. Peak modal gain and Peak optical gain with Current density for $In_{0.29}Ga_{0.71}As_{0.99}N_{0.01}$/GaAs straddled heterostructures.

The optical gain is the fundamental characteristics of the quantum well heterostructures' based lasers. According to the theory of density matrix, the optical gain can be determined by summing up contribution from overall transitions in between the electrons and holes in the conduction and valence sub-bands, respectively. The optical gain which depends on the confinement factor, GRIN (graded refractive index) layers and number of quantum wells is termed as modal gain [33]. For $In_{0.29}Ga_{0.71}As_{0.99}N_{0.01}$/GaAs Straddled Heterostructures, the behaviours of optical gain and modal gain in terms of lasing wavelength are plotted on the left (black) and right (blue) y-axes, respectively in Fig. 2. In the both spectra of optical gain and modal gain, two peaks are observed. Occurring of the upper peak is due to transition between electrons associated with the first conduction subband and heavy hole subband; while the lower peak is obtained due to the second conduction subband and heavy hole subband. The maximum optical gain and modal gain are obtained of the order of ~2100 cm^{-1} and 20 cm^{-1}, respectively, at a lasing wavelength of 1.30 μm, as shown in Fig. 2. Actually, the lasing heterostructures emitting the radiations in the wavelengths of ~1.3 μm have generated great interest for applications in optical fiber communications because the 1.3 μm wavelength is attractive due to zero dispersion in the silica based optical fiber. For these reasons, it is important to have a light emitter heterostructure which can operate at wavelengths of 1.3.

Taking into account the interest on InGaAlAs/InP heterostructure that shows a peak gain at 1.55 μm (preferred wavelength for minimum optical loss), the optical gain characteristics of InGaAsN/GaAs heterostructure have been compared with the InGaAlAs/InP heterostructure. Both of these structures are of same geometry. Figure 3exhibits comparative optical gain spectra for the same carrier concentrations (~$2 \times 10^{18} cm^{-3}$) between InGaAsN/GaAs and InGaAlAs/InP straddled heterostructures. In case of InGaAsN/GaAs heterostructure, the obtained maximum optical gain (i.e., ~2100 cm^{-1} at 1.30 μm) is almost half of the maximum optical gain (i.e. ~4200 cm^{-1} at 1.55 μm) of InGaAlAs/InP straddled heterostructures. In addition, for both of these heterostructures, transparency wavelengths have also been compared. In Fig. 3, it can be seen that the proposed InGaAsN/GaAs nano-heterostructure exhibits low transparency wavelength (of the order of ~0.93 μm) as compared to the transparency wavelength (~1.19 μm) of InGaAlAs/InP heterostructure, hence proposed InGaAsN/GaAs heterostructure has low transparency and threshold condition rather than those in InGaAlAs/InP heterostructure. The non linear behaviour of peak modal gain and peak optical gain with current density for $In_{0.29}Ga_{0.71}As_{0.99}N_{0.01}$/GaAs straddled heterostructures is also shown in Fig. 4. In Fig. 4, it can be seen that for any value of current density the obtained peak optical gain is approximately more than hundred times of peak modal gain.

The spectrum knowledge of refractive index of QWs in the heterostructure has a vital role in the design and implementation of nano-scale opto-electronic equipments. In a past literature, it has been reported that a quantum-well laser have a higher gain and a smaller refractive-index change than a conventional diode laser [34]. For the heterostructure, the most important differences between quantum well or active region and barrier layers (SCH region) occur normally in the energy of band-gap and the index of refraction. The variation in the energy band-gap permits spatial confinement of injection carriers of electrons and holes in the conduction and valence bands; while the variations in index of refraction can be used to develop the optical waveguides, hence, it is very essential to determine the explicitly of a refractive index change with the carrier density in the quantum region of the nano-scale heterostructure. Refractive index change and peak optical gain with carrier density for $In_{0.29}Ga_{0.71}As_{0.99}N_{0.01}$/GaAs straddled heterostructures are plotted within right and left y-axes, respectively, in Fig. 5. In the lower carrier density regime, Figure 5 shows that the refractive index change and peak optical gain exhibit inversely behaviour with carrier density, while for higher carrier density region both the refractive index change and peak optical gain exhibit proportional behaviour with carrier density.

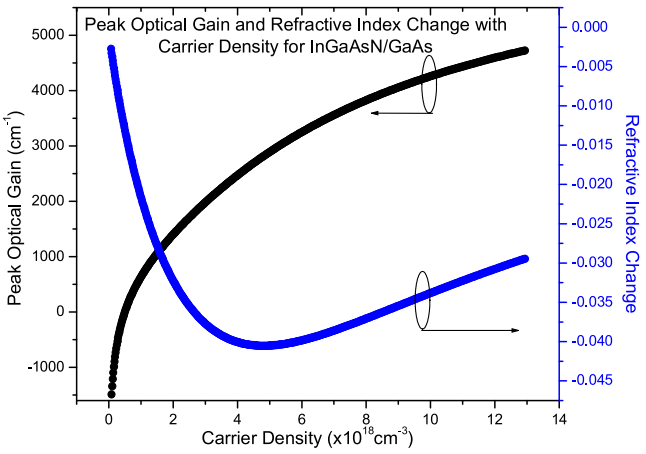

Fig. 5. Peak optical gain and refractive index change gain with Carrier density for $In_{0.29}Ga_{0.71}As_{0.99}N_{0.01}$/GaAs straddled heterostructures.

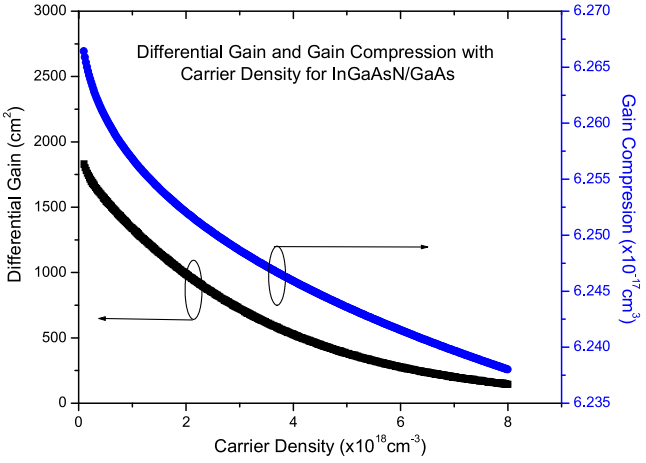

Fig. 6. Differential gain and Gain compression with Carrier density for $In_{0.29}Ga_{0.71}As_{0.99}N_{0.01}$/GaAs straddled heterostructures.

The derivative of optical gain with respect to carrier density is known as differential gain. It plays an important role in determining the characteristics of a quantum well based lasing heterostructure. The gain compression factor (also known as gain suppression or gain saturation or non linear gain coefficient) is substantial parameter to design properly of QW lasing structures. This factor can also be used in shaping the amplitude and frequency modulation of the lasing diodes. In general, the linear gain does not dependent of the density of photon. However, at upper photonic densities, the gain tends to reduce; this reduction behaviour of gain is termed as gain compression. The gain compression is basically caused by the depletion of electrons at fixed energy levels due to strong stimulated recombination or spectral holes burning. Basically, QW-lasing heterostructure performs above the threshold condition; in this condition the saturation mechanism and small fluctuations of relative intensity of output light are occurred, this type of saturation mechanism is called gain compression. An approximately similar reciprocal behaviour of differential gain and gain compression with carrier density on left (black) and right (blue) axes, respectively, for $In_{0.29}Ga_{0.71}As_{0.99}N_{0.01}$/GaAs straddled heterostructures is shown in Fig. 6. In addition to the optical gain, the differential gain and anti-guiding factor are substantial parameters in the dynamics performance of quantum well heterostructures based lasers. The anti-guiding factor plays a very crucial role in deciding the optical gain of lasing heterostructure and can be defined in terms of refractive index change and differential gain. The differential gain and anti-guiding factor are plotted with carrier density for $In_{0.29}Ga_{0.71}As_{0.99}N_{0.01}$/GaAs straddled heterostructures on right and left axes, respectively in Fig. 7. Figure 7 shows the proportional and reciprocal behaviours of anti-guiding factor and differential gain, respectively as a function of carrier density.

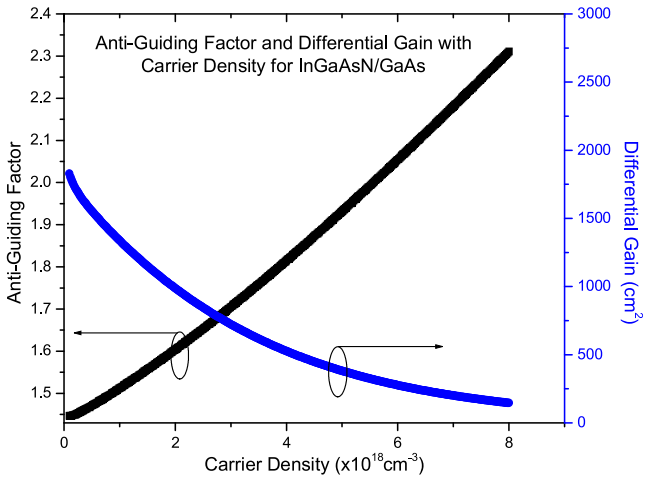

Fig. 7. Anti-Guiding factor and Differential gain with Carrier density for $In_{0.29}Ga_{0.71}As_{0.99}N_{0.01}$/GaAs straddled heterostructures.

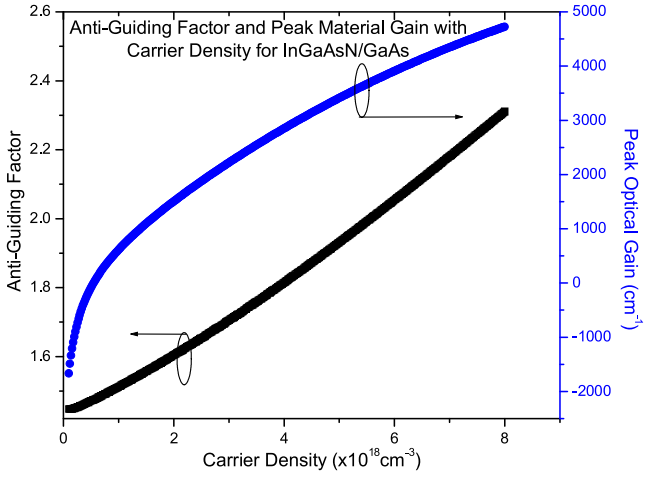

Fig. 8. Anti-guiding factor and Peak Optical gain with Carrier density for $In_{0.29}Ga_{0.71}As_{0.99}N_{0.01}$/GaAs straddled heterostructures.

In general, the anti-guiding factor supports in obtaining the optical gain because both have proportional behaviour with carrier density, this proportional behaviours of anti-guiding factor and peak optical gain with carrier density for $In_{0.29}Ga_{0.71}As_{0.99}N_{0.01}$/GaAs straddled heterostructures are shown in Fig. 8. Next, the behaviour of peak optical gain and leakage current with carrier density for $In_{0.29}Ga_{0.71}As_{0.99}N_{0.01}$/GaAs straddled heterostructures is exhibited in Fig. 9. In Fig. 9 it is shown that, the leakage current approximately remains same at low value of carrier density, while at higher value of carrier density it increases drastically. Leakage current and anti-guiding factor with carrier density for $In_{0.29}Ga_{0.71}As_{0.99}N_{0.01}$/GaAs straddled heterostructures are plotted in Fig. 10. Relaxation oscillation frequency (ROF) and optical output power have important role in the determination of threshold current. The fixed value of current at which relaxation oscillation frequency and optical output power both are obtained negligible is called threshold current. Basically, above the threshold current the optical gain occurs positive while below the threshold current it becomes negative. The relaxation oscillation frequency and

Table 3
Comparison of InGaAsN/GaAs heterostructure with the various heterostructure reported till date.

S. No.	Different Quantum Well Heterostructures with Material Composition	Type	Well Width(Å)	Optical Gain (/cm)	Lasing Wavelength (μm)	References
1	$In_{0.45}Ga_{0.55}As/GaAs_{0.31}\ Sb_{0.69}$ (M-shaped)	II	60	1000	2.6	[36]
2	$In_{0.71}Ga_{0.21}Al_{0.08}As/InP$	I	60	4200	1.55	[37,38]
3	$Al_{0.10}Ga_{0.90}As/GaAs$	I	60	3800	0.83	[39]
4	$In_{0.90}Ga_{0.10}As_{0.59}P_{0.41}/InP$	I	60	7600	1.40	[40]
5	$In_{0.53}Ga_{0.47}As/GaAs_{0.51}Sb_{0.49}$ (W-shaped)	II	50	1600	1.98	[41]
6	$In_{0.70}Ga_{0.30}As/GaAs_{0.40}Sb_{0.60}$ (M-shaped)	II	40	9000	1.95	[28]
7	$In_{0.25}Ga_{0.75}As/InAs/GaAs_{0.31}Sb_{0.69}$ (W-shaped) (with two QWs)	II	20	4800	3.2	[42]
8	$Al_{0.75}Ga_{0.25}N/GaN/Al_{0.65}Ga_{0.35}N$	II	30	3500	0.245	[43]
9	$Al_{0.92}In_{0.8}N/GaN/\ Al_{0.92}In_{0.8}N$	II	20	2750	0.263	[44]
10	$In_{0.29}Ga_{0.71}As_{0.99}N_{0.01}/GaAs$	I	40	2100	1.3	Present Work

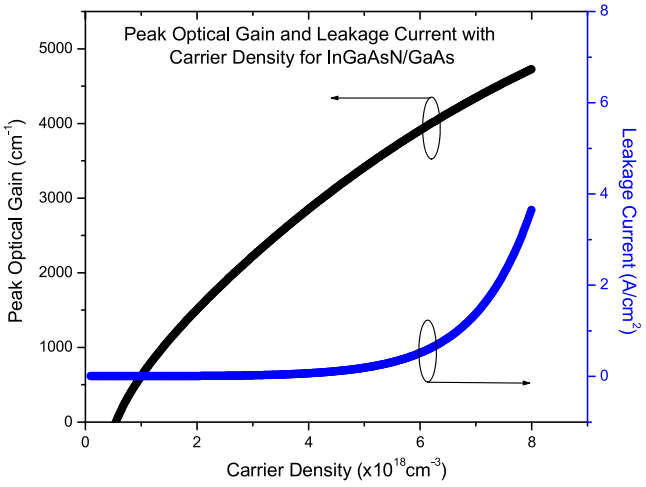

Fig. 9. Peak optical gain and Leakage current with Carrier density for $In_{0.29}Ga_{0.71}As_{0.99}N_{0.01}/GaAs$ straddled heterostructures.

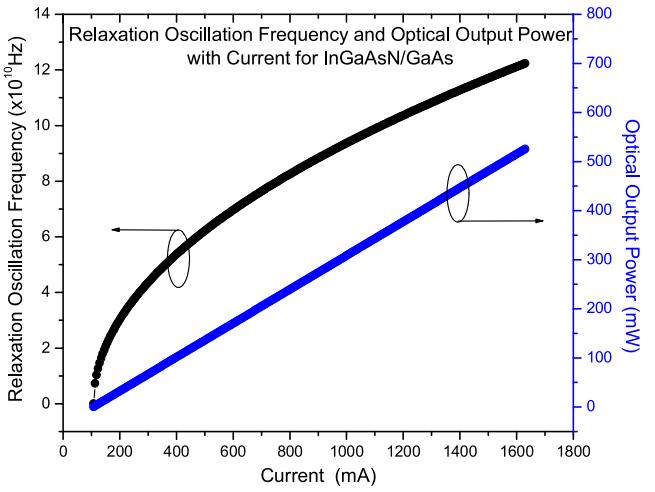

Fig. 11. Relaxation oscillation frequency and optical output power with current $In_{0.29}Ga_{0.71}As_{0.99}N_{0.01}/GaAs$ straddled heterostructures.

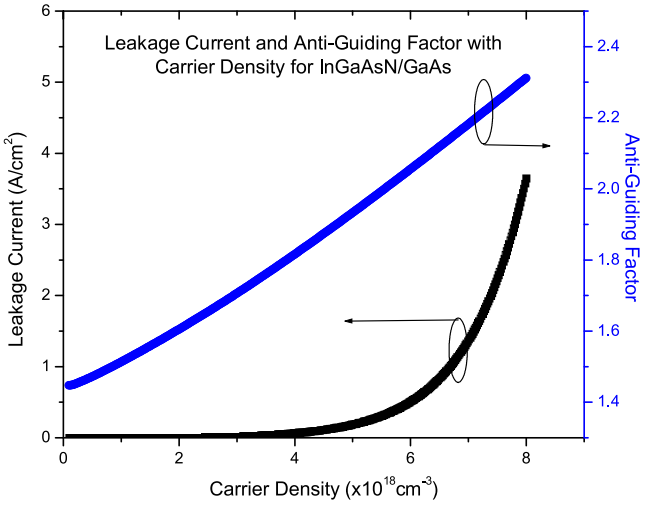

Fig. 10. Leakage current and Anti-guiding factor with Carrier density for $In_{0.29}Ga_{0.71}As_{0.99}N_{0.01}/GaAs$ straddled heterostructures.

optical output power with current for $In_{0.29}Ga_{0.71}As_{0.99}N_{0.01}/GaAs$ straddled heterostructures are plotted on left and right y-axes, respectively, in Fig. 11. In Fig. 11, the optical output power and relaxation oscillation frequency do not exist at current of 100 mA (threshold current). It is clear by curves of Fig. 11, above the threshold current, the optical output power and relaxation oscillation frequency both are enhanced with the increase in current. For a 200 mA current, the relaxation oscillation frequency is almost 30 GHz which is comparable to the ROF of GaAs/GaAlAs multiple quantum well (MQW) lasing heterostructure [35]. Moreover, the behaviour of optical power is exactly linear with the current while the behaviour of ROF with the current is not linear. In order to make the comparison of InGaAsN/GaAs nano-heterostructure with other various heterostructure, the data are collected, compared and analyzed in Table 3. In Table 3, it can be seen that the InGaAsN/GaAs based heterostructure exhibits the maximum gain within the NIR region. Therefore, $In_{0.29}Ga_{0.71}As_{0.99}N_{0.01}/GaAs$ based heterostructure is very suitable for the generation of radiations within NIR wavelength region. On analysis of Table 3, the gain and lasing wavelength of InGaAsN/GaAs heterostructure can be compared with those of InGaAlAs/InP heterostructure. On comparison, it is found that the maximum optical gain of InGaAsN/GaAs heterostructure is almost half of the maximum optical gain of InGaAlAs/InP straddled heterostructures. Although the maximum gain of InGaAsN/GaAs heterostructure is almost half of the gain of InGaAlAs/InP heterostructure, but from the wavelength point of view the InGaAsN/GaAs nano-heterostructure is also more desirable because the 1.3 μm wavelengths is attractive due to negligible dispersion in the silica based optical fiber. Hence, the InGaAsN/GaAs nano-heterostructure can be very valuable in optical fiber based communication systems. Other specific applications

of InGaAsN/GaAs nano-heterostructure may be in Infrared vibrational spectroscopy (or near-infrared spectroscopy), in the thin film metrology, in climatology, in the infrared cleaning and in the study of biological systems.

4. Conclusions

For the InGaAsN/GaAs nano-heterostructure, eight band Kohn-Luttinger Hamiltonian has been solved to determine the wavefunctions associated with the valence subbands (i.e., heavy and light holes) and their corresponding discrete energies within the frame work of GAIN simulation package that works in the vicinity of the zone centre at the Γ point. The optical and lasing properties of InGaAsN/GaAs nano-heterostructure have been determined and compared with the InGaAlAs/InP heterostructure. In comparison, it is found that the gain of InGaAs/GaAs is almost half of the gain of InGaAlAs/InP heterostructure, but from the wavelength point of view the InGaAsN/GaAs nano-heterostructure is also more desirable because the 1.3 μm wavelength is attractive due to a negligible dispersion in the silica based optical fiber. Hence, the InGaAsN/GaAs nano-heterostructure can be very valuable in optical fiber based communication systems.

Acknowledgements

P. A. Alvi, Sandhya K, Pyare Lal, Garima Bhardwaj and Richa Dolia are grateful to “Banasthali Center for Research and Education in Basic Sciences” under CURIE programme supported by the DST, Government of India, New-Delhi. Authors are also thankful to Dr. Konstantin I. Kolokolov (Physics Department, Moscow State University, Moscow, Russia) for technical support.

References

[1] S. Nakamura, S. Pearton, G. Fasol, The Blue Laser Diode, Springer, Berlin, 2000.
[2] A. Kuramata, K. Domen, R. Soejima, K. Horino, S. Kubota, T. Tanahashi, InGaN laser diode grown on 6H–SiC substrate using low-pressure metal organic vapor phase epitaxy, Jpn. J. Appl. Phys. 36 (1997) L1130.
[3] J.K. Sheu, F.W. Huang, C.H. Lee, M.L. Lee, Y.H. Yeh, P.C. Chen, W.C. Lai, Improved conversion efficiency of GaN-based solar cells with Mn-doped absorption layer, Appl. Phys. Lett. 103 (2013), 063906.
[4] F.Y. Wu, P.B. Keller, D. Kapolnek, P.S. Denbaars, U.K. Mishra, Measured microwave power performance of AlGaN/GaN MODFET, IEEE Electron. Dev. Lett. 17 (1995) 455–457.
[5] F.Y. Wu, P.B. Keller, P. Parikh, D. Kapolnek, S.P. Denbaars, U.K. Mishra, Bias dependent microwave performance of AlGaN/GaN MODFET's up to 100 V, IEEE Electron. Dev. Lett. 18 (1997) 290–292.
[6] Z.I. Alferov, The history and future of semiconductor heterostructures, Semiconductors 32 (1998) 1.
[7] P.A. Alvi, Sapna Gupta, Meha Sharma, Swati Jha, F. Rahman, Computational modeling of novel InN/$Al_{0.30}In_{0.70}N$ multilayer nano-heterostructures, Phys. E: Low.-Dimens. Syst. Nanostruct. 44 (2011) 49–55.
[8] P.A. Alvi, Strain compensated InN based superlattice, Adv. Sci. Lett. Vol. 5 (17) (2012) 101–107.
[9] Sapna Gupta, F. Rahman, M.J. Siddiqui, P.A. Alvi, Strain profile in III-nitride based multilayer nano-heterostructures, Phys. B: Condens. Matter 411 (2013) 40–47.
[10] Y.S. Park, Wide bandgap III-nitride semiconductors: opportunities for future optoelectronics, Optoelectron. Rev. 9 (2) (2001) 117–124.
[11] S. Yoshida, S. Misawa, S. Gonda, Improvements on the electrical and luminescent properties of reactive molecular beam epitaxially grown GaN films by using AlN-coated sapphire substrates, Appl. Phys. Lett. 42 (1983) 427.
[12] S. Nakamura, M. Senoh, T. Mukai, Si-Doped InGaN films grown on GaN films, Jpn. J. Appl. Phys. 32 (1993) L8–11.
[13] S. Nakamura, M. Senoh, S. Nagahama, N. Iwasa, T. Yamada, T. Matsushita, H. Kiyoku, Y. Sugimoto, InGaN-based multi-quantum-well-structure laser diodes, Jpn. J. Appl. Phys. 35 (1996) L74.
[14] A. Khan, M.J.N. Kuzina, D.T. Olson, W.J. Schaff, J.W. Burm, M.S. Shur, Microwave performance of a 0.25 μm gate AlGaN/GaN heterostructure field effect transistor, Appl. Phys. Lett. 65 (1994) 1121–1122.
[15] X.Q. Shen, T. Ide, M. Shimizu, H. Okumura, High-quality InGaN/GaN multiple quantum wells grown on Ga-polarity GaN by plasma-assisted molecular-beam epitaxy, J. Appl. Phys. 89 (2001) 5731.
[16] H.M. Ng, T.D. Moustakas, K.F. Ludwig Jr, Structural and optical characterization of InGaN/GaN multiple quantum wells grown by molecular beam epitaxy, J. Vac. Sci. Technol. B 18 (2000) 1457.
[17] S.B. Che, Y. Ishitani, A. Yoshikawa, Fabrication and characterization of 20 periods InN/InGaN MQWs, Phys. Status Solidi C 3 (2006) 1953.
[18] A. Reklaitis, Terahertz-frequency InN/GaN heterostructure-barrier varactor diodes, J. Phys.: Condens. Matter 20 (2008), 384202.
[19] K.T. Tsen, C. Poweleit, D.K. Ferry, H. Lu, W.J. Schaff, Observation of large electron drift velocities in InN by ultrafast raman spectroscopy, Appl. Phys. Lett. 86 (2005), 222103.
[20] M. Razeghi, A. Rogalski, Semiconductor ultraviolet detectors, J. Appl. Phys. 79 (1996) 7433.
[21] D.B. Jackrel, S.R. Bank, H.B. Yuen, M.A. Wistey, J.S. Harris, A.J. Ptak Jr, S.W. Johnston, D.J. Friedman, S.R. Kurtz, Dilute nitride GaInNAs and GaInNAsSb solar cells by molecular beam epitaxy, J. Appl. Phys. 101 (2007), 114916.
[22] A. Härkönen, J. Rautiainen, M. Guina, J. Konttinen, P. Tuomisto, L. Orsila, M. Pessa, O. Okhotnikov, High power frequency doubled GaInNAs semiconductor disk laser emitting at 615 nm, Opt. Express 15 (2007) 3224–3229.
[23] S. Calvez, J. Hastie, M. Guina, O. Okhotnikov, M. Dawson, Semiconductor disk laser for the generation of visible and ultraviolet radiation, Laser Photon. Rev. 3 (2009) 407–434.
[24] V.-M. Korpijärvi, M. Guina, J. Puustinen, P. Tuomisto, J. Rautiainen, A. Härkönen, A. Tukiainen, O. Okhotnikov, M. Pessa, MBE grown GaInNAs-based multi-watt disk lasers, J. Cryst. Growth 311 (2009) 1868–1871.
[25] H. Riechert, A.Yu. Egorovtt, D. Livshitst, B. Borchert, S. Illek, InGaAsN/GaAs Heterostructures for Long-Wavelength Light-Emitting Devices”, 8th Int. Symp. “Nanostructures: Physics and Technology, St Petersburg, Russia, 2000, June 19-23.
[26] H.K. Nirmal, S.G. Anjum, Pyare Lal, Amit Rathi, S. Dalela, M.J. Siddiqui, P.A. Alvi, Field effective band alignment and optical gain in type-I $Al_{0.45}Ga_{0.55}As/GaAs_{0.84}P_{0.16}$ nano-heterostructures, Optik 127 (2016) 7274–7282.
[27] S.L. Chuang, Physics of Optoelectronic Devices, Wiley, New York, 1995.
[28] H.K. Nirmal, Nisha Yadav, F. Rahman, P.A. Alvi, Optimization of high optical gain in type-II $In_{0.70}Ga_{0.30}As/GaAs_{0.40}Sb_{0.60}$ lasing nano-heterostructure for SWIR applications, Superlattices Microstruct. 88 (2015) 154–160.
[29] H.K. Nirmal, Nisha Yadav, S. Dalela, Amit Rathi, M.J. Siddiqui, P.A. Alvi, Tunability of optical gain (SWIR region) in type-II In0.70Ga0.30As/GaAs0.40Sb0.60 nano-heterostructure under high pressure, Phys. E 80 (2016) 36–42.
[30] P.A. Alvi, Transformation of type-II InAs/AlSb nanoscale heterostructure into type-i structure and improving interband optical gain, Phys. Status Solidi B 254 (No. 5) (2017), 1600572.
[31] S.L. Chung, Physics of Photonic Devices, 2nd edition, Willey & Sons, Inc., 2009.
[32] W. Lin-Zhang, T. Wei, G. Feng, Determination of quasi fermi-level separation of semiconductor lasers from amplified spontaneous emission, Chin. Phys. Lett. Vol. 21 (No.7) (2004) 1359–1361.
[33] P.A. Alvi, P. Lal, R. Yadav, S. Dixit, S. Dalela, Modal gain characteristics of GRIN-InGaAlAs/InP lasing nano-heterostructures, Superlattice Microstruct. 61 (2013) 1–12.
[34] W.W. Chow, D. Depatie, Carrier-induced refractive-index change in quantum-well lasers, Opt. Lett. Vol. 13 (4) (1988) 303–305.
[35] K. Uomi, T. Mishima, N. Chinone, Ultrahigh relaxation oscillation frequency (up to 30 GHz) of highly p-doped GaAs/GaAlAs multiple quantum well lasers, Appl. Phys. Lett. 51 (1987) 78.
[36] B. Chen, W.Y. Jiang, A.L. Holmes Jr, Design of strain compensated InGaAs/GaAsSb type-II quantum well structures for mid-infrared photodiodes, Opt. Quant Electron. 44 (2012) 103–109.
[37] P.A. Alvi, Pyare Lal, S. Dalela, M.J. Siddiqui, An extensive study on simple and GRIN SCH-based $In_{0.71}Ga_{0.21}Al_{0.08}As$/InP lasing heterostructures, Phys. Scr. 85 (2012), 035402.
[38] P.A. Alvi, Strain-induced non-linear optical properties of straddling-type indium gallium aluminum arsenic/indium phosphide nanoscale-heterostructures, Mater. Sci. Semicond. Process Vo. 31 (2015) 106–115.
[39] P. Lal, S. Dixit, F. Rahman, P.A. Alvi, Gain simulation of lasing nano-heterostructure $Al_{0.10}Ga_{0.90}As/GaAs$, Phys. E: Low-Dimens. Syst. Nanostruct. 46 (2012) 224–231.
[40] R. Yadav, P. Lal, F. Rahman, S. Dalela, P.A. Alvi, Investigation of material gain of $In_{0.90}Ga_{0.10}As_{0.59}P_{0.41}$/InP lasing nano-heterostructure, Int. J. Mod. Phys. B Vol. 28 (No. 10) (2014), 1450068.
[41] C.H. Pan, C.P. Lee, Design and modeling of InP-based InGaAs/GaAsSb type-II “W” type quantum wells for mid-infrared laser applications, J. Appl. Phys. 113 (2013), 043112.
[42] N. Yadav, G. Bhardwaj, S.G. Anjum, S. Dalela, M.J. Siddiqui, P.A. Alvi, Investigation of high optical gain in complex type-II InGaAs/InAs/GaAsSb nano-scale heterostructure for MIR applications, Appl. Opt. 56 (May (15)) (2017).
[43] J. Zhang, N. Tansu, Engineering of AlGaN-delta-GaN quantum-well gain media for mid- and deep-ultraviolet lasers, IEEE Photon. J. Vol. 5 (No.2) (2013), 2600209.
[44] C.-K. Tan, W. Sun, D. Borovac, N. Tansu, Large optical gain AlInN-delta-GaN quantum well for deep ultraviolet emitters, Sci. Rep. 6 (2016), 22983.